Selective Distribution of Surface-Modified TiO2 Nanoparticles in Polystyrene-b-poly (Methyl Methacrylate) Diblock Copolymer

ARTICLE *in* CHEMISTRY OF MATERIALS · JUNE 2003

Impact Factor: 8.35 · DOI: 10.1021/cm0300617

2 AUTHORS, INCLUDING:

Kung-Hwa Wei
National Chiao Tung University
172 PUBLICATIONS **6,219** CITATIONS

Selective Distribution of Surface-Modified TiO_2 Nanoparticles in Polystyrene-b-poly (Methyl Methacrylate) Diblock Copolymer

Chin-Cheng Weng and Kung-Hwa Wei*

Department of Materials Science and Engineering, National Chiao Tung University, Hsinchu, Taiwan 30049 Republic of China

Received April 10, 2003

Ordered aggregates of surfactant-modified TiO_2 nanoparticles in the selective block of lamellar assemblies of the diblock copolymer PS-b-PMMA have been prepared. The hydrophobic or hydrophilic nature of the tethered surfactant determines the location of TiO_2 nanoparticles in the corresponding block, as confirmed by transmission electron microscopy, differential scanning calorimetry, and Fourier transform infrared spectroscopy. The modes of dispersion of TiO_2 in the blocks depend on the type of bonding between the surfactant and TiO_2. Photoluminescence studies of these nanocomposites demonstrate that the location of TiO_2 nanoparticles affect the block copolymer's luminescence at different wavelengths.

Introduction

Owing to their optical and electrical properties, semiconductor nanoparticles or clusters are emerging materials and have the potential to be used in a wide range of applications.[1,2] For semiconductor or metal oxide nanoparticles with sizes close to their Bohr radius (typically between 1 and 10 nm), the size-dependent band gap results in tunable optical properties.[1] Nanoparticles that are not treated with a surfactant or bonded to polymer chains will, however, form large aggregates. Furthermore, optoelectronic devices require nanoparticles to form ordered, one- to three-dimensional structures.[3]

Block copolymers (BCPs) are a versatile platform material because they can self-assemble into various periodic structures for proper compositions and under adequate conditions, owing to the microphase separation between dissimilar blocks.[4,5] A diblock copolymer, the simplest case, self-assembles into various equilibrium morphologies, such as alternating layers, complex topologically connected cubic structures, cylinders on hexagonal lattices, and spheres on a body-centered lattice. Self-assembly of BCPs can therefore serve as templates for the spatial arrangement of nanoparticles in thin films or in bulk samples and can provide an effective means to manipulate their positions.

In recent years, much effort has been directed toward the synthesis of semiconductor or metal oxide nanoparticles within block copolymer matrix materials.[6−16] For instance, BCPs/semiconductor nanoparticle nanocomposites have been synthesized for applications involving photonic band gap devices.[17,18] Studies using ZnS,[7,10,11] PbS,[6,8,9] and CdS[7,12−14] within BCPs and CdS in salt-induced BCPs micelles[15,16] have also been reported. Among these studies, the common approach has been to synthesize the nanocrystal clusters within microphase-separated diblock copolymer films by attaching metal complexes to the functionalized block of the copolymer before microdomain formation. Then, the composite block copolymers are treated with hydrogen sulfur gases for obtaining nanoparticles in situ. Although the functional groups in the monomer that are used to bind the metals can be designed appropriately for one block of the copolymer, variations within the nanocrystal cannot be easily controlled within the microdomains of the block copolymers. Furthermore, these functionalized block copolymers are not suitable for use as large area templates, as opposed to the more readily available block copolymers such as polystyrene-b-poly (methyl methacrylate) (PS-b-PMMA) or polystyrene-b-poly (ethylene oxide) (PS-b-PEO). In the present study we have adopted an approach of synthesizing nanoparticles with modified surfactants. The surfactant can be either hydrophilic or hydrophobic, with one of its ends tethered

* To whom correspondence should be addressed. Tel: 886-35-731871. Fax: 886-35-724727. E-mail: khwei@cc.nctu.edu.tw.

(1) Henglein, A. *Chem. Rev.* **1989**, *89*, 1861.
(2) Wang, Y.; Herron, N. *J. Phys. Chem.* **1991**, *95*, 525.
(3) Murry, C. B.; Kagan, C. R.; Bawendi, M. G. *Science* **1995**, 270.
(4) Bates, F. S. *Science* **1991**, *251*, 898.
(5) Thomas, E. L. *Science* **1999**, *286*, 1307.
(6) Sankaran, V.; Cummins, C. C.; Schrock, R. R.; Cohen, R. E.; Silbey, R. J. *J. Am. Chem. Soc.* **1990**, *112*, 6858.
(7) Cummins, C. C.; Schrock, R. R.; Cohen, R. E. *Chem. Mater.* **1992**, *4*, 27.
(8) Kane, R. S.; Cohen, R. E.; Silbey, R. *Chem. Mater.* **1996**, *8*, 1919.
(9) Tassoni, R.; Schrock, R. R. *Chem. Mater.* **1994**, *6*, 744.
(10) Yue, J.; Sankaran, V.; Cohen, R. E.; Schrock, R. R. *J. Am. Chem. Soc.* **1993**, *115*, 4409.
(11) Sankaran, V.; Yue, J.; Cohen, R. E. *Chem. Mater.* **1993**, *5*, 1133.
(12) Moffitt, M.; Eisenberg, A. *Chem. Mater.* **1995**, *7*, 1178
(13) Moffitt, M.; McMahon, L.; Pessel, V.; Eisenberg, A. *Chem. Mater.* **1995**, *7*, 1185.
(14) Moffitt, M.; Vali, H.; Eisenberg, A. *Chem. Mater.* **1998**, *10*, 1021.
(15) Zhao, H.; Douglas, E. P.; Harrison, B. S.; Schanze, K. S. *Langmuir* **2001**, *17*, 8428.
(16) Zhao, H.; Douglas, E. P. *Chem. Mater.* **2002**, *14*, 1418.
(17) Fink, Y.; Urbas, A. M.; Bawendi, M. G.; Joannopoulos, J. D.; Thomas, E. L. *J. Lightwave Technol.* **1999**, *17*, 1963.
(18) Edrington, A. C.; Urbas, A. M.; DeRege, P.; Chen, C. X.; Swager, T. M.; Hadjichristidis, N.; Xenidou, M.; Fetters, L. J.; Joannopoulos, J. D.; Fink, Y.; Thomas, E. L. *Adv. Mater.* **2001**, *13*, 421.

10.1021/cm0300617 CCC: $25.00
Published on Web 06/17/2003

Scheme 1. Synthesis of TiO_2 Nanoparticles by Ionic or Nonionic Surfactants

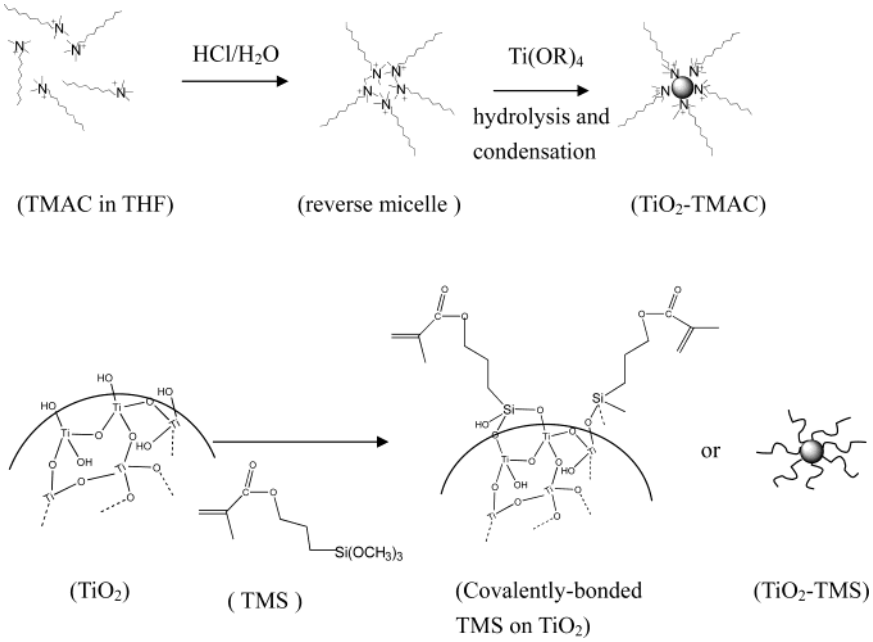

Table 1. Compositions of TiO_2 Colloidal Solutions

	THF (mL)	TMAC (g)	TMS (g)	H_2O (g)	HCl (g) (36%)	TTIP/IPA (mL)
TiO_2−TMAC in THF	5	0.085		0.05	0.026	0.5
TiO_2−TMS in THF	5		0.016	0.05	0.026	0.5
TiO_2−H^+ in THF	5			0.05	0.026	0.5

to a nanoparticle by an ionic bond or a covalent bond. The selective dispersion of these nanoparticles in one block of the diblock copolymer through either van der Waals or polar interactions between the particular block and the surfactants without altering the chemical structure of the diblock copolymer is desired. This selectivity is important in designing the optical properties of nanoparticles−block copolymer hybrid systems. For instance, in a diblock copolymer, nanoparticles can be placed into blocks with the higher refractive index for enlarging the differences between the refractive indices of the two blocks for photonic crystal application.[17,18]

Here, we report on dispersing surfactant-modified TiO_2 nanoparticles into either block of a PS-b-PMMA diblock copolymer with an ordered lamellar phase. TiO_2 was first synthesized in tetrahydrofuran (THF) instead of in a water or alcohol phase.[19−21] Cetyl trimethylammonium chloride (TMAC) amphiphilics or 3-(methacryloyloxypropyl)-trimethoxy silane (TMS) surfactant was used to modify the TiO_2 nanoparticles. To our knowledge, this presents a new approach to selectively disperse quantum-confined nanoparticles in a PS-b-PMMA diblock copolymer with an ordered lamellar phase.

Experimental Section

Materials. Polystyene-*block*-polymethyl methacrylate (PS-b-PMMA) diblock copolymer was purchased from Polymer Source, Inc. The polydispersity index, M_w/M_n, was 1.12, and the number-average molecular weights (M_n) of the PS and PMMA blocks were 85 000 and 91 000 g/mol, respectively, as determined by SEC. Cetyl trimethylammonium chloride (TMAC) was obtained from Taiwan Surfactant, Inc. 3-(Methacryloyloxypropyl)-trimethoxy silane (TMS, 97%) was obtained from Lancaster. Titanium tetra (isopropoxide) (TTIP, 98%, Acros USA), isopropyl alcohol (IPA, 99.9%, TEDIA), THF (99.0%, Pharmco USA), and HCl (36%, Acros) were obtained from commercial sources.

Synthesis of TiO_2 Nanoparticles. Reagent-grade chemicals and solvents were used without further purification. The precursor TTIP was diluted to 0.1 M with IPA (TTIP/IPA). The TiO_2−TMAC and TiO_2−H^+ colloidal solutions were prepared by mixing TMAC, HCl, and deionized water in THF for 30 min. Afterward, TTIP/IPA was dropped in slowly with rapid stirring. The compositions of these TiO_2 colloidal solutions are given in Table 1. The TiO_2−H^+ colloidal solution was then put in a vacuum oven at 65 °C for solvent removal. Subsequently, a light yellow powder was obtained. TiO_2−TMS colloidal solution was first prepared with HCl, deionized water, and TTIP/IPA. TMS was added to the solution after 2 h. The synthesis of surfactant-modified TiO_2 nanoparticles is shown in Scheme 1.

Preparation of TiO_2/PS-b-PMMA Nanocomposites. A 0.1-g aliquot of PS-b-PMMA was added to 5 mL of TiO_2−TMAC, TiO_2−H^+, or TiO_2−TMS colloidal solutions. After the mixture was stirred for 3 h, it was transferred to a Petri dish and organic solvent was removed at 65 °C for 12 h.

Characterization. Transmission electron microscopy (TEM) studies were carried out on a JEOL 2000FX electron microscope operating at 200 keV. The samples for TEM studies were prepared by directly dispersing the TiO_2 solution on a carbon film supported on a holey copper grid. Ultrathin sections of TiO_2/PS-b-PMMA for TEM studies were deposited on copper grids after microtoning with a Leica ultracut Uct. The morphologies of all the bulk films were obtained by TEM after cutting a roughly 100-nm thin film. Energy-dispersive X-ray scattering (EDS) spectra were taken on a Link ISIS (OXFORD)

(19) Kormann, C.; Bahnemann, D. W.; Hoffmann, M. R. *J. Phys. Chem.* **1988**, *92*, 5196.
(20) Joselevich, E.; Willner, I. *J. Phys. Chem.* **1994**, *98*, 7628.
(21) Serpone, N.; Lawless, D.; Khairutdinov, R. *J. Phys. Chem.* **1995**, *99*, 16646.

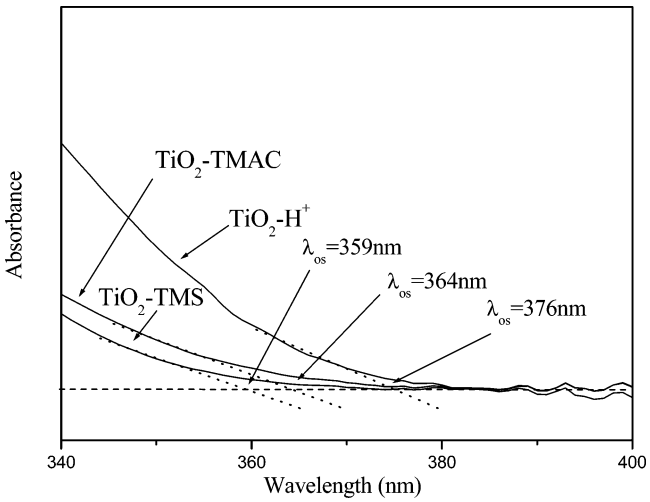

Figure 1. UV−vis absorbance spectra of TiO_2 colloidal solutions.

detector connected to the electron microscope. UV−vis absorption spectra were obtained on an Aglient 8453 UV−vis spectroscopy system by scanning between 190 and 1000 nm. The nanosized TiO_2 colloidal solutions were diluted to 6×10^{-5} M for the UV−vis experiment. From the spectral absorption edge (λ_{os}), the diameters of the TiO_2 nanoparticles were calculated by using absorption onset data.[19] The X-ray diffraction study was carried out with a MAC Science MXP 18 X-ray diffractometer (50 kV, 40 mA) with copper target and Ni filter at a scanning rate of 4°/min. The glass transition temperatures (T_g) of the bulk films were obtained from a Dupont DSC 2910 at a heating rate of 20 °C/min. Fourier transform infrared spectroscopy (FTIR) spectra of the samples were obtained using a Nicolet PROTÉGÉ-460. The photoluminescence of TiO_2/PS-b-PMMA was observed under excitation of the sample by UV light at 260 nm, in air, with a Hitachi F4500 fluorescence spectrophotometer at room temperature. The ^{29}Si solid-state NMR spectrum was recorded with a Bruker DMX-600 NMR spectrometer.

Results and Discussion

Figure 1 shows the UV−vis spectra of TiO_2−TMAC, TiO_2−H^+, and TiO_2−TMS solutions. The concentration of TiO_2 nanoparticles in both colloidal solutions is about 6×10^{-5} M. The shifts in the UV−vis absorption onset of these TiO_2 colloidal solutions suggest that the TiO_2 nanoparticles have quantum-confined properties.[22,23] The reference absorption and the corresponding band gap energy are $\lambda_{ref} = 385$ nm and $Eg_{ref} = 3.2$ eV (we assume an anatase crystal shape for TiO_2 in the calculation). From the onset absorption wavelength (λ_{os}), the radii of the TiO_2 particles were calculated using eq 1.

$$Eg_{os} - Eg_{ref} = \Delta Eg \approx \frac{\hbar^2\pi^2}{2R^2} \times \frac{1}{\mu} - \frac{1.8e^2}{\epsilon R} \qquad (1)$$

Here, R is the radius of the particle, μ is the reduced mass of the exciton (i.e., $\mu^{-1} = m_h^{*-1} + m_e^{*-1}$, where m_e^* is the effective mass of the electron and m_h^* is the effective mass of the hole), and ϵ is the dielectric constant of the material. Here, we use mean values of $\mu = 1.63m_e$ and $\epsilon = 184$ for the calculation.

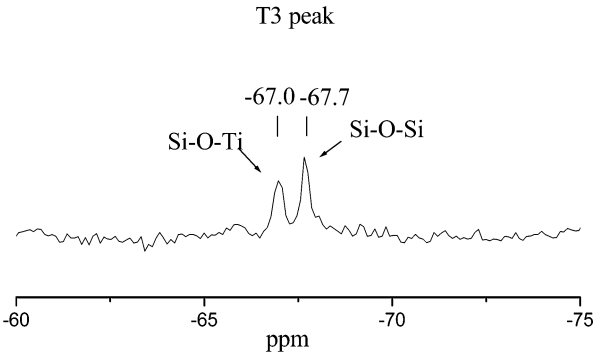

Figure 2. ^{29}Si NMR spectrum of the TiO_2−TMS colloidal solution.

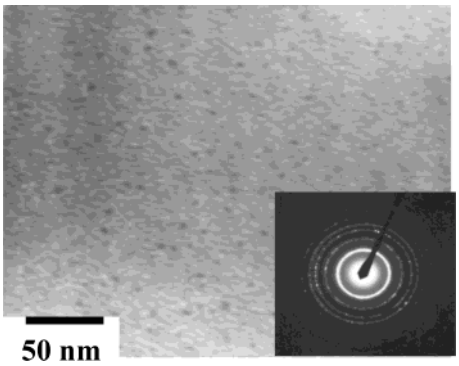

Figure 3. Transmission electron microscopy image and electron diffraction pattern of TiO_2 nanoparticles from TiO_2−H^+ colloidal solution.

Table 2. Onset of UV−Vis Absorbance and Calculated Radii of TiO_2 Nanoparticles

	absorbance onset wavelength (nm)	radius (nm)
TiO_2−TMAC	359	0.96
TiO_2−TMS	364	1.07
TiO_2−H^+	376	1.59

Table 2 shows the calculated radii of TiO_2 particles in the colloidal solutions. The growth of TiO_2 particles by the sol−gel reaction is catalyzed by acid, and, therefore, the TiO_2−H^+ colloidal solution has the largest TiO_2 radius (1.59 nm) among all colloidal solutions. The sizes of TiO_2 in TiO_2−TMAC and TiO_2−TMS are similar (0.96 and 1.07 nm), but the stabilities of the solutions are different. After being stirred for 36 h, the TiO_2−TMAC and TiO_2−H^+ colloidal solutions became muddy after an initially being transparent yellow-brown. The TiO_2−TMS solution, however, remained transparent after 36 h stirring, and became light yellow and transparent after 45 days. This phenomenon indicates that the covalently bonded surfactant (TMS) effectively prevents TiO_2 particles from aggregating. Figure 2 shows the ^{29}Si NMR spectrum of TiO_2−TMS. The spectrum shows a T^3 peak, resulting from the bonding structure of [$Si(OSi)_3R$], at −67 ppm.[24−26] There is no presence of a T^1 peak, which would originate from a ($RSi(OSi)(OR')_2$) structure, at −45 ppm or a T^2 peak, from a ($RSi(OSi)_2(OR')_1$) structure, at −57 ppm. This indicates that most of the Si−OH groups of TMS react

(22) Brus, L. *J. Phys. Chem.* **1986**, *90*, 2555.
(23) Liu, Y.; Claus, O. *J. Am. Chem. Soc.* **1997**, *119*, 5273.
(24) Isdoa, K.; Kuroda, K. *Chem. Mater.* **2000**, *12*, 1702.
(25) Delattre, L.; Babonneau, F. *Chem. Mater.* **1997**, *9*, 2385.
(26) Leu, C. M.; Wu, Z. W.; Wei, K. H. *Chem. Mater.* **2002**, *14*, 3016.

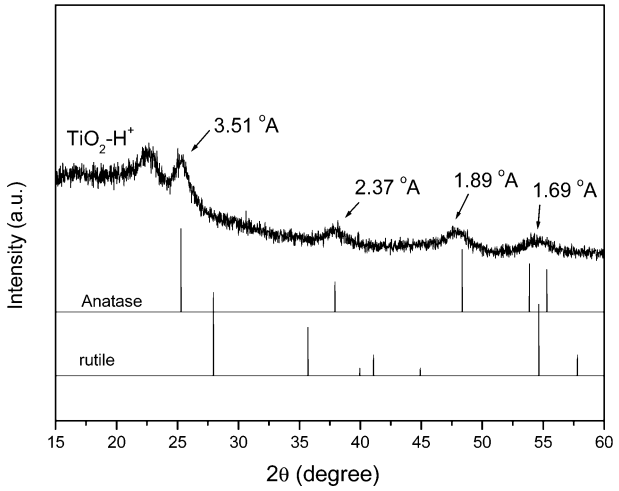

Figure 4. X-ray diffraction curve of TiO_2-H^+ nanoparticles.

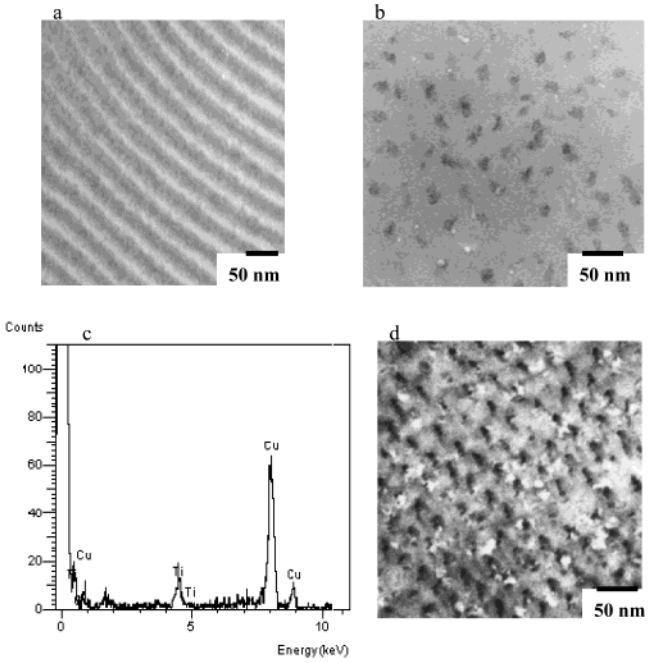

Figure 5. Transmission electron microscopy images of (a) PS-b-PMMA, (b) $TiO_2-TMAC/PS-b-PMMA$, and (d) $TiO_2-TMAC/PS-b-PMMA$ stained with RuO_4. (c) Shows an energy-dispersive X-ray diffraction pattern of the dark particles in (b).

to give Si−O−M (M = Si or Ti). The splitting of the T^3 peak (−67.0and −67.7 ppm) implies that TMS is attached to TiO_2 by a covalent bond. The TEM image of TiO_2-H^+ in Figure 3 indicates that the particle size is about 3 nm, which is also the value estimated by eq 1. Figure 4 shows the X-ray diffraction curve of TiO_2-H^+ nanoparticles, and the TiO_2 nanoparticles are determined to have an anatase phase, which has partial crystallinity. The diffraction pattern of TiO_2 particles on a carbon grid is shown in the bottom-right corner of Figure 3 and indicates that the TiO_2 particles are partially crystalline.

Morphology and Photoluminescence of TiO_2/PS-b-PMMA. Figure 5(a) shows the lamellar morphology of PS-b-PMMA after staining with RuO_4. The periodic lamellar thickness of PS-b-PMMA is about 50 nm. The dark region is the PS domain, owing to staining, and the PS volume fraction of PS-b-PMMA is 0.55, which

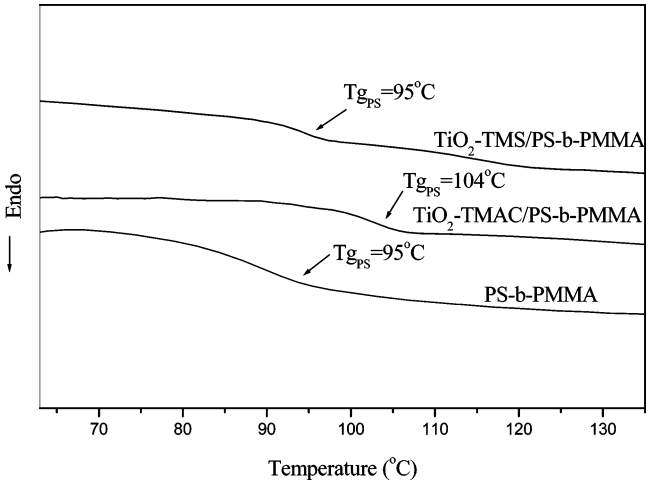

Figure 6. Differential scanning calorimetry curves of PS-b-PMMA, $TiO_2-TMS/PS-b-PMMA$, and $TiO_2-TMAC/PS-b-PMMA$.

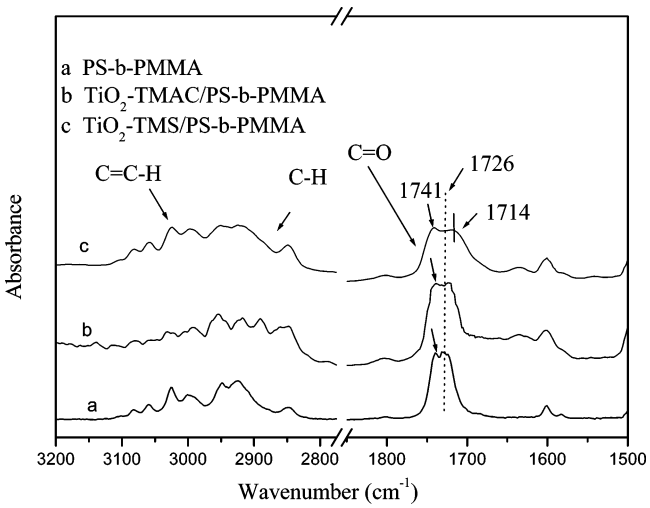

Figure 7. Fourier transform infrared spectra of PS-b-PMMA and TiO_2/PS-b-PMMA nanocomposites.

falls into the ordered lamellar phase region[4] (a PS volume fraction between 0.34 and 0.62). The $TiO_2-TMAC/PS-b-PMMA$ morphology is shown in Figure 5(b). In Figure 5(b), the presence of TiO_2 in the dark spots is confirmed by EDS (Figure 5(c)); the size of TiO_2 aggregates (dark spots) is about 15−20 nm. The Ti band peak indicates the existence of TiO_2 at the PS domains, whereas the presence of Cu peaks is caused by the Cu grid used in the sample preparation. In Figure 5(d), the gray phase is the PS domain, which is a result of staining with RuO_4, while the light phase is the PMMA domain. Dark TiO_2 nanoparticles are found to disperse in the gray domain (PS domain) in the lamellar PS-b-PMMA. That the TiO_2-TMAC nanoparticles can be dispersed in the PS domain corresponds to the fact that both the cetyl trimethylammonium chloride (TMAC), containing 10 methylene units, and the polystyrene domain are hydrophobic and miscible. The presence of TiO_2-TMAC in the PS domain is further supported by differential scanning calorimetry (DSC) results. Figure 6 reveals that the glass transition temperature (T_g) of the PS domain in $TiO_2-TMAC/PS-b-PMMA$ increased by 9 °C, as compared to that of neat PS-b-PMMA (104 °C vs 95 °C). This increase might be attributed to TiO_2 aggregates, which hinder the molecular movement of

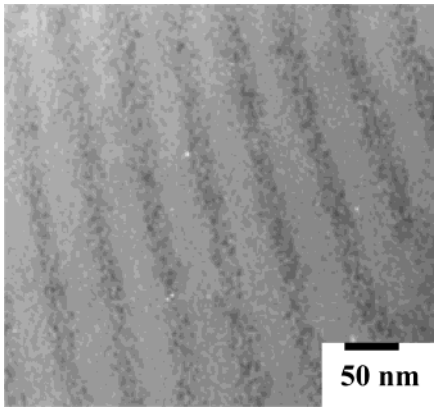

Figure 8. Transmission electron microscopy image of TiO_2−TMS/PS-b-PMMA.

the PS domain, indicating that TiO_2−TMAC aggregates are located at the PS domain. Because the heat capacity of glass transition of PMMA is much smaller than that of PS (0.03 W/g vs 0.065 W/g), the Tg of PMMA is indetectable in this case.[27] Therefore, the presence of TiO_2 in the PMMA phase of PS-b-PMMA can only be confirmed by other means. The Fourier transform infrared (FTIR) spectra of TiO_2/PS-b-PMMA nanocomposites are shown in Figure 7. The peaks at 1741 cm^{-1} and 1726 cm^{-1} result from the carbonyl groups of the PMMA domain in neat PS-b-PMMA. The carbonyl band of TiO_2−TMS/PS-b-PMMA shifts to lower wavenumbers (from 1726 to 1714 cm^{-1}) as compared to that of PS-b-PMMA. This indicates the possibility that TiO_2 is present in the PMMA domain because hydrogen bonding between the remainder of the dangling −OH groups on the surface of TiO_2 and the carbonyl groups of the PMMA domains causes the carbonyl band to shift to smaller wavenumbers. Figure 8 shows a transmission electron microscopy image of TiO_2−TMS/PS-b-PMMA. That the TiO_2 nanoparticles are dispersed rather uniformly in the PMMA phase is consistent with the fact that TMS contains methacrylate structures. The difference in the modes of dispersion of TiO_2 in PS and in PMMA domains can be manifested by the bonding difference between the surfactants and TiO_2. In the TiO_2−TMAC/PS-b-PMMA case, the polar-ionic bondings between TiO_2 surfaces and TMAC are weak and hence allow TiO_2 nanoparticles to rearrange to form aggregates during the solvent removal process. Whereas in the TiO_2−TMS/PS-b-PMMA case, TMS is bonded to TiO_2 surfaces covalently, and this type of bonding is well maintained during the solvent removal process. The covalently tethered TMS prevents TiO_2 from aggregating, resulting in a better dispersion. A schematic drawing of the formation of these two types of dispersion of TiO_2 in the PS and PMMA block is presented in Figure 9.

Figure 10 shows the photoluminescence of the TiO_2/PS-b-PMMA nanocomposites as excited by 260 nm UV light. A mild 410 nm luminescence peak, caused by the band-to-band transition,[24] is displayed by the TiO_2 nanoparticles modified by TMS. For neat PS-b-PMMA, the 320 nm luminescence peak is resulted from the PS domain. In the case of TiO_2−TMAC/PS-b-PMMA, only a broad and weak 326 nm luminescence peak appeared. Whereas in the case of TiO_2−TMS/PS-b-PMMA, there are two luminescence peaks (323 and 400 nm) present. The stark difference in the two cases can be interpreted by the morphological evidences as discussed in the previous paragraph. When TiO_2−TMAC forms aggregates in the PS domain, a large portion of the excitation light is absorbed by the PS domain, which also luminesces at shorter wavelength, resulting in a small portion of excitation light reaching TiO_2 aggregates.

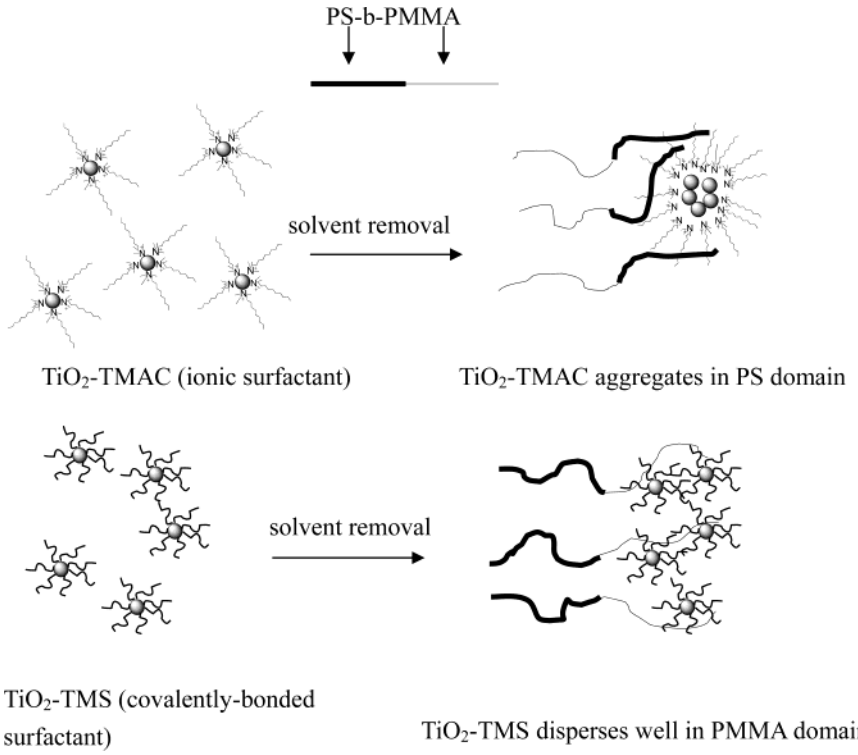

Figure 9. Schematic drawing of different dispersion modes by ionic-polar and covalent bondings between TiO_2 and surfactants in PS-b-PMMA.

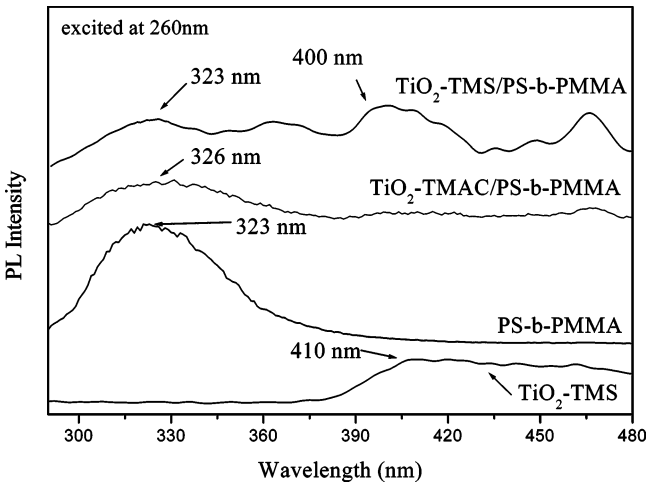

Figure 10. Photoluminescence of TiO_2−TMS, PS-b-PMMA, and TiO_2/PS-b-PMMA nanocomposites.

This results in nonluminescence by TiO_2−TMAC in the PS domains. On the other hand, because TiO_2−TMS nanoparticles dispersed more uniformly in the PMMA domain, both TiO_2−TMS nanoparticles and the PS domain can luminescence independently. This luminescence phenomenon is consistent with our previous argument on the distribution of TiO_2 nanoparticles in different blocks.

Conclusion

The dispersion of TiO_2 nanoparticles can be controlled in one of the two blocks of lamellar PS-b-PMMA by using hydrophobic or hydrophilic surfactants, as revealed by transmission electron microscopy, differential scanning calorimetry, and Fourier transform infrared spectroscopy. The modes of dispersion of TiO_2 nanoparticles in different blocks are determined by the type of bondings between the surfactant and the nanoparticles. The photoluminescence of the TiO_2/PS-b-PMMA nanocomposites depends on the location of the TiO_2 nanoparticles.

Acknowledgment. We appreciate the financial support of the National Science Council, Taiwan, through project NSC 91-2120-M-009-001.

CM0300617

(27) Guegan, P.; Cernohous, J. J.; Khandpur, A. K.; Hoye, T. R.; Macosko, C. W. *Macromolecules* **1996**, *29*, 4605.